Research Article Vol. 9, No. 7 / 1 July 2019 / Optical Materials Express 3109
Optical Materials EXPRESS

Polycrystalline diamond photonic waveguides realized by femtosecond laser lithography

HAISSAM HANAFI,[1,*] SEBASTIAN KROESEN,[1] GEORGIA LEWES-MALANDRAKIS,[2] CHRISTOPH NEBEL,[2] WOLFRAM H. P. PERNICE,[3] AND CORNELIA DENZ[1]

[1]*Institute for Applied Physics, University of Münster, Corrensstr. 2, 48149 Münster, Germany*
[2]*Fraunhofer Institute for Applied Solid State Physics, Tullastr. 72, 79108 Freiburg, Germany*
[3]*Institute of Physics, University of Münster, Heisenbergstr. 11, 48149 Münster, Germany*
[*]*E-mail: haissam.hanafi@uni-muenster.de*

Abstract: In recent years, the perception of diamond has changed from it being a pure gemstone to a universal high-tech material. In the field of photonics, an increased interest is emerging due to its outstanding optical properties, such as its high refractive index, a spectrally wide transmission window, and high Raman coefficient. Furthermore, the capability to host color defects for room temperature single photon generation makes diamond an attractive platform for quantum photonics. Known as *nature's hardest material*, the fabrication and handling of crystalline diamond for integrated optics remains challenging. Here, we report on the fabrication of three-dimensional Type III depressed cladding waveguides in polycrystalline diamond substrates by direct laser writing. Single mode waveguiding is demonstrated in the near-infrared telecommunication C-band. We believe that this enables the fabrication of three-dimensional large-scale photonic circuits, which are essential for advanced classical and quantum diamond photonics.

1. Introduction

Integrated optical systems allow combining highly optimized photonic building blocks into functional circuits with small footprints and reproducible characteristics [1]. Their inherent stability and scalability make them particularly attractive for applications in telecommunications [2,3], metrology [4,5] and sensing [6,7]. Besides wide-spread use in classical optics, nanophotonic circuits are also gaining increased relevance for quantum photonic applications due to their potential of operating in the single photon regime [8–10]. Building on established fabrication routines transferred from microelectronics, photonic circuits are nowadays realized with high yield and reproducibility. Because sub-wavelength devices are often required, electron beam lithography with subsequent dry etching is a frequently used approach for realizing such photonic devices [11]. Yet these fabrication procedures lead to quasi-planar geometries and prevent access to the third dimension which is required for advanced optical components such as broadband polarizers, three-dimensional photonic crystals or functional metamaterials. New lithography techniques which enable arbitrary geometries to be devised in three-dimensions are increasingly sought after. Direct laser writing (DLW) is among the most promising approach for generating three-dimensional photonic structures. Voxel-wise addressing provides the means to create photonic devices which contain both in-plane and out-of-plane components and are therefore out of reach for traditional planar fabrication techniques. While DLW removes restrictions on the desired geometry, the combination with functional materials is still challenging because to date DLW is carried out predominantly in organic polymers, glass or crystalline materials [12–17]. This in general limits the operational wavelength range of the devices based on DLW,

#364723 https://doi.org/10.1364/OME.9.003109
Journal © 2019 Received 15 Apr 2019; revised 15 May 2019; accepted 16 May 2019; published 24 Jun 2019

Optical Materials EXPRESS

and also may lead to reduced mechanical stability in the case of polymeric structures. In order to extend material options, inversion-based strategies have been developed to transfer organic resist structures to other materials using atomic layer deposition and infiltration techniques. Alternatively, DLW can be carried out directly in transformable materials which inherently provide the desired material characteristics.

Here, we break new grounds in a different direction: we implement DLW in large-scale polycrystalline diamond samples and demonstrate functional waveguides allowing single mode guiding in the near-infrared wavelength regime at the telecommunication C-band. Previous studies on waveguide fabrication with DLW were limited to single crystal diamond [18–21]. Even though single crystal substrates offer a high purity, the fabrication of large samples is challenging and limits its applications. Polycrystalline diamond in contrast can be fabricated in wafer-like sizes with high optical quality and reproducibility at low cost compared to single diamond substrates. Furthermore, the ability to grow large-area polycrystalline diamond thin films on different insulating substrates as for instance SiO_2, makes it attractive for on-chip photonic circuits [22,23]. To date diamond photonic devices have exclusively been fabricated using planar nanofabrication to realize a range of photonic components including optical cavities, photonic crystals, optomechanical resonators and frequency combs. However, the recent interest in three-dimensional quantum photonic structures such as quantum simulators exploiting Boson sampling, random walk structures and coupled waveguide devices requires appropriate fabrication tools that enable true three-dimensional integration. Our approach allows combining the geometric flexibility of DLW with the material advantages of polycrystalline diamond to yield a rich platform for broadband operational photonic circuitry. The use of polycrystalline diamond for DLW holds promise for both classical and quantum photonic systems to be realized in a flexible and scalable fashion.

2. Methods

Diamond substrate fabrication: Direct laser writing was carried out on polycrystalline diamond substrates prepared by microwave plasma enhanced chemical vapor deposition (PECVD) in ellipsoidal cavity reactors with a microwave frequency of 2.45 GHz. CVD diamond layers with thicknesses of 300 µm were grown on silicon templates and afterwards surface treated by chemomechanical polishing. After dissolving the silicon template, the diamond layers were laser-diced into 3×3 mm^2 pieces.

Waveguide fabrication in polycrystalline diamond: Type III depressed cladding waveguides were fabricated using a femtosecond Ti-sapphire laser system (Coherent Legend) with a central wavelength of 800 nm, a pulse duration of 115 fs and a repetition rate of 1 kHz. Focusing the laser pulse into the diamond substrate by using a high numerical aperture (NA) microscope objective (Nikon 100x, 0.8 NA) exceeds the field for non-linear absorption and results in permanent structural modification [24]. Three-dimensional permanent structures are induced by moving the sample with a high-precision translation stage (Aerotech ALS 130H) relative to the beam focus (c.f. Figs. 1(b) and (c)). A sketch of the induction scheme is displayed in Fig. 1(a). Previous studies which have identified the structural modification by Raman-spectroscopy arising from diamond-graphite phase transitions leads to a highly localized tensile stress in the surrounding area [25]. This enables the fabrication of Type III depressed cladding waveguides, allowing both, s- and p-polarized light guiding [19,26,27]. Note that due to so called filamentation [28] and spherical aberration, caused by a refractive index mismatch of air and the diamond substrate we obtain axially elongated filaments. This in general can be overcome by applying costly adaptive optics techniques to compensate for the arising aberrations. Here, to induce the desired waveguide profile, the geometrical dimensions of the elongated filaments are analyzed with respect to the writing pulse energy and the nominally addressed depth. Single filaments are then placed on an ellipse forming the desired circular waveguide core. Each waveguide consists of

Optical Materials EXPRESS

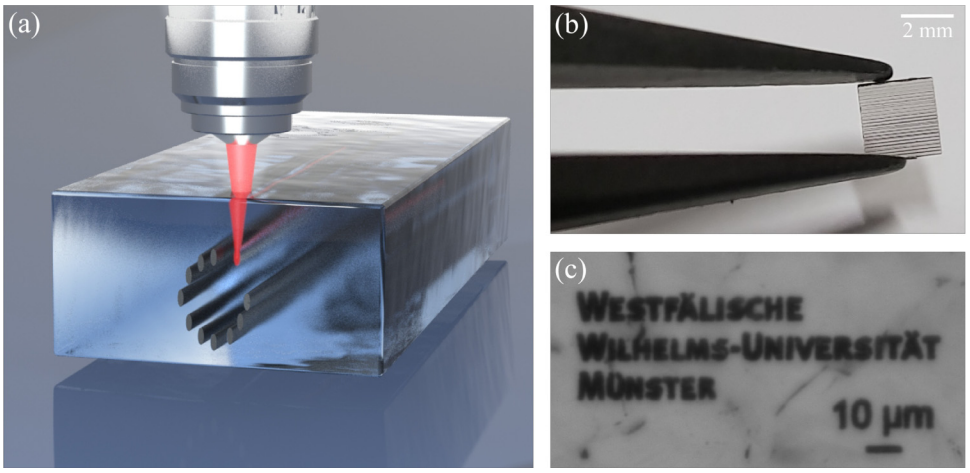

Fig. 1. Three-dimensional diamond photonic waveguide fabrication: (a) sketch of the scheme, (b) photography of the processed sample exhibiting numerous waveguide structures, (c) bright-field transmission image of an exemplary laser-induced material modification inside the diamond substrate.

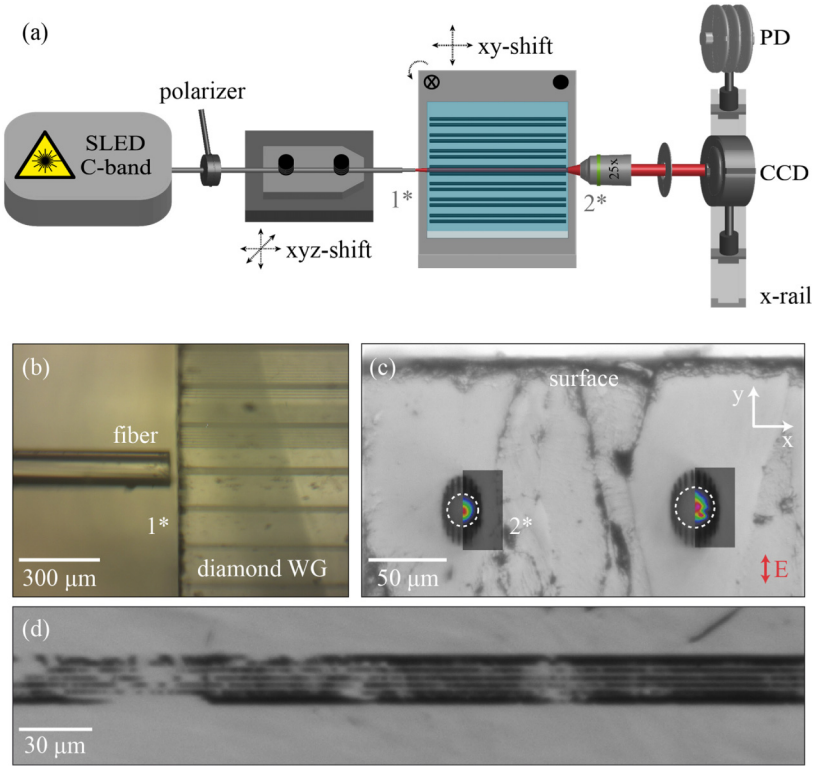

Fig. 2. Three-dimensional diamond photonic waveguide characterization: (a) schematic of the characterization setup (for simplicity the microscope at the sample position is not illustrated), (b) top view microscope image at the front-facet depicting the cleaved SMF28 fiber and the processed diamond sample, (c) end-facet of the type III depressed cladding waveguides, over layered with the measured guided near-field mode profile for a core diameter of 20 µm and 25 µm, (d) top view microscope image of a fabricated waveguide.

Optical Materials EXPRESS

approximately 20 individual filaments. The waveguide structures are induced 90 µm beneath the substrate surface. We have successfully achieved optimal induction conditions of our waveguide structures by performing an extensive parameter scan with respect to the propagation properties for pulse energies between 20 nJ to 30 nJ at a scanning speed of 30 µm/s.

Waveguide characterization: The induced waveguide structures are analyzed in the near-infrared C-band by a superluminescent diode (SLED). The laser light is guided by a SMF28 fiber from the source and fiber-butt coupled to the laser written diamond photonic waveguides (c.f. Fig. 2(b)). A fiber squeezer controls the polarization of the laser light which is set to vertical polarization. The processed sample is mounted on a 4-Axis stage enabling translation in the x- and y-directions and the correction of the polar and azimuthal tilts. The guided near field profile is imaged by a microscope objective (Melles Griot 25x, 0.5 NA) onto a CCD camera (c.f. Fig. 2(c)). After replacing the camera with a photodiode (PD) the transmitted intensity is measured and the insertion losses are characterized. A pinhole in front of the PD prevents unguided light hitting the detector. A sketch of the full characterization set up is depicted in Fig. 2(a).

3. Results and discussion

We have investigated the guided mode profiles and insertion losses of laser-induced diamond waveguides for several fabrication parameters including induction pulse energies and waveguide core diameters. To calibrate the system with respect to the spatial dimensions and to control the quality of the excitation laser beam, we measured the mode profile guided by the SMF28 fiber (c.f. Fig. 3(c1)). The observed mode profile is Gaussian shaped and suitable to excite the fabricated diamond waveguides. For a waveguide having a core diameter of 20 µm induced with a pulse energy of 20 nJ, we observed single mode guiding with an overall insertion loss of -16.4 dB (c.f. Fig. 3(a1)). Increasing the core diameter to 25 µm leads to multimode guiding (c.f. Fig. 3(b1)). Furthermore, we note a decrease in the insertion loss of 30%. Keeping the core diameter constant at 20 µm and increasing the induction pulse energy to 25 nJ we do not find a significant change in insertion losses but multimode guiding with two *hot spots* (c.f. Fig. 3(a2)). Increasing the pulse energy further to 30 nJ results in an increased loss of 12% retaining a multimode guiding behavior

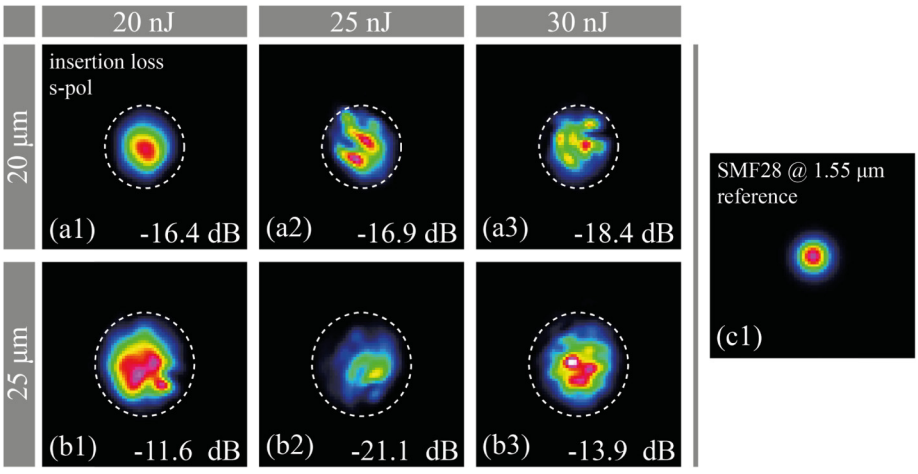

Fig. 3. Measured near-field mode profile for vertically polarized laser light at 1550 nm (a) for a waveguide core diameter of 20 µm and (b) 25 µm for induction energies reaching from (a1,b1) 20 nJ to (a3,b3) 30 nJ, (c1) near-field mode profile of the SMF28 fiber acting as a reference to calibrate the system.

Optical Materials EXPRESS

(c.f. Fig. 3(a3)). Keeping the core diameter constant at 25 µm and increasing the induction pulse energy to 25 nJ reveals dramatically higher insertion losses of 80% (c.f. Fig. 3(b2)). When increasing the pulse energy to 30 nJ, the insertion losses are 20% higher compared to an induction energy of 20 nJ. For a larger core diameter, lower coupling losses are expected, resulting in lower insertion losses which is in good accordance with the experimental results. We found waveguides with a core diameter of less than 20 µm not being able to guide light. This can be ascribed to the cutoff wavelength for the given modulation strength. Furthermore, we note a dependence of the guiding properties on the induction energy. On the one hand the insertion losses increase for higher induction energies. On the other hand a change from single mode guiding to multi-mode guiding is observed. An increased pulse energy is expected to induce a higher tensile stress field which leads to an increased effective refractive index modulation. This in general decreases the propagation losses due to a higher mode confinement. Moreover, stronger material modifications originating from higher induction pulse energies in the waveguide core cause higher absorption and scattering which reduces the transmittance. In our realizations, we observe the latter case to be predominant. An exception is found for a waveguide induced with a pulse energy of 25 nJ and a core diameter of 25 µm. This may be caused by spatial inhomogeneities in the polycrystalline diamond substrate resulting in a non-uniform threshold characteristic along the waveguide as seen in Fig. 2(d). Additionally, the polished front facet shows absorbing tracks (c.f. Fig. 2(c)) which leads to a decreased coupling efficiency. This is not related to the material quality nor the fabrication method but can be simply improved by an additional polishing of the front facet.

4. Conclusions

In conclusion we showed polycrystalline diamond to be a versatile material for full three-dimensional integrated optical circuitry. It can be effectively modified by femtosecond DLW to yield photonic waveguides. Compared to DLW in single crystal diamond our approach allows the fabrication of large-scale diamond photonic circuits. Using DLW enables arbitrary optical components to be realized in thick diamond samples. Besides full flexibility in designing optical circuits, the use of DLW enables structuring large-scale samples made from bulk CVD diamond, thus avoiding nucleation-related defects and surface contamination. Buried waveguides also allow for incorporating deep color defects directly into waveguiding networks which will be attractive for diamond quantum photonics and the realization of high-quality single photon emitters on a chip [29,30]. Individual color defects could be identified prior to DLW and then being interconnected with customized waveguides into single photon networks. Furthermore, the wide spectral transparency window of diamond enables ultra-broadband waveguide devices to be realized within a single material. As diamond provides optical transparency into the far infrared region DLW paves this way to access the unexplored wavelength regimes and make it become accessible for photonics computing chips [20].

Funding

Deutsche Forschungsgemeinschaft (DFG) (PE 1832/5-1); University of Muenster.

Acknowledgements

W.H.P. Pernice acknowledges support by the Deutsche Forschungsgemeinschaft (DFG) through grant PE 1832/5-1. We acknowledge support from the Open Access Publication Fund of the University of Muenster.

References

1. A. F. Koenderink, A. Andrea, and P. Albert, "Nanophotonics: shrinking light-based technology," Science **348**(6234), 516–521 (2015).
2. R. Kirchaina and L. Kimerling, "A roadmap for nanophotonics," Nat. Photonics **1**(6), 303–305 (2007).

Optical Materials EXPRESS

3. J. Pfeifle, V. Brasch, M. Lauermann, Y. Yu, D. Wegner, T. Herr, K. Hartinger, P. Schindler, J. Li, D. Hillerkuss, R. Schmogrow, C. Weimann, R. Holzwarth, W. Freude, J. Leuthold, T. J. Kippenberg, and C. Koos, "Coherent terabit communications with microresonator Kerr frequency combs," Nat. Photonics **8**(5), 375–380 (2014).
4. J. A. Liddle and G. M. Gallatin, "Lithography, metrology and nanomanufacturing," Nanoscale **3**(7), 2679–2688 (2011).
5. P. O'Brien, M. K. Smit, and C. Koos, "Special issue on 'integrated photonic devices: sensors, materials, systems'," Adv. Opt. Technol. **4**(2), 117–118 (2015).
6. A. B. Dahlin, N. J. Wittenberg, F. Höök, and S. H. Oh, "Promises and challenges of nanoplasmonic devices for refractometric biosensing," Nanophotonics **2**(2), 83–101 (2013).
7. M. C. Estevez, M. Alvarez, and L. M. Lechuga, "Integrated optical devices for lab-on-a-chip biosensing applications," Laser Photonics Rev. **6**(4), 463–487 (2012).
8. A. Politi, J. C. F. Matthews, M. G. Thompson, and J. L. O'Brien, "Integrated quantum photonics," IEEE J. Sel. Top. Quantum Electron. **15**(6), 1673–1684 (2009).
9. J. L. O'Brien, A. Furusawa, and J. Vučković, "Photonic quantum technologies," Nat. Photonics **3**(12), 687–695 (2009).
10. A. Politi, M. J. Cryan, J. G. Rarity, S. Yu, and J. L. O'Brien, "Silica-on-silicon waveguide quantum circuits," Science **320**(5876), 646–649 (2008).
11. A. Kaganskiy, M. Gschrey, A. Schlehahn, R. Schmidt, J. H. Schulze, T. Heindel, A. Strittmatter, S. Rodt, and S. Reitzenstein, "Advanced in-situ electron-beam lithography for deterministic nanophotonic device processing," Rev. Sci. Instrum. **86**(7), 073903 (2015).
12. N. F. Hasselmann, M. J. Hackmann, and W. Horn, "Two-photon fabrication of hydrogel microstructures for excitation and immobilization of cells," Biomed. Microdevices **20**(1), 8 (2018).
13. S. Kroesen, K. Tekce, J. Imbrock, and C. Denz, "Monolithic fabrication of quasi phase-matched waveguides by femtosecond laser structuring the χ (2) nonlinearity," Appl. Phys. Lett. **107**(10), 101109 (2015).
14. R. R. Gattass and E. Mazur, "Femtosecond laser micromachining in transparent materials," Nat. Photonics **2**(4), 219–225 (2008).
15. G. Della Valle, R. Osellame, and P. Laporta, "Micromachining of photonic devices by femtosecond laser pulses," J. Opt. A: Pure Appl. Opt. **11**(1), 013001 (2009).
16. H. B. Sun and S. Kawata, "Two-photon photopolymerization and 3D lithographic microfabrication," *NMR • 3D Analysis • Photopolymerization*, Springer, Berlin, Heidelberg, 169–273 (2004).
17. J. Imbrock, H. Hanafi, M. Ayoub, and C. Denz, "Local domain inversion in MgO-doped lithium niobate by pyroelectric field-assisted femtosecond laser lithography," Appl. Phys. Lett. **113**(25), 252901 (2018).
18. B. Sotillo, V. Bharadwaj, J. P. Hadden, M. Sakakura, A. Chiappini, T. T. Fernandez, S. Longhi, O. Jedrkiewicz, Y. Shimotsuma, L. Criante, R. Osellame, G. Galzerano, M. Ferrari, K. Miura, R. Ramponi, P. E. Barclay, and S. M. Eaton, "Diamond photonics platform enabled by femtosecond laser writing," Sci. Rep. **6**(1), 35566 (2016).
19. A. Courvoisier, M. J. Booth, and P. Salter, "Inscription of 3D waveguides in diamond using an ultrafast laser," Appl. Phys. Lett. **109**(3), 031109 (2016).
20. V. Bharadwaj, Y. Wang, T. T. Fernandez, R. Ramponi, S. M. Eaton, and G. Galzerano, "Femtosecond laser written diamond waveguides: A step towards integrated photonics in the far infrared," Opt. Mater. **85**, 183–185 (2018).
21. P. Rath, N. Gruhler, S. Khasminskaya, C. Nebel, C. Wild, and W. H. P. Pernice, "Waferscale nanophotonic circuits made from diamond-on-insulator substrates," Opt. Express **21**(9), 11031–11036 (2013).
22. F. Lenzini, N. Gruhler, N. Walter, and W. H. P. Pernice, "Diamond as a Platform for Integrated Quantum Photonics," Adv. Quantum Technol. **1**(3), 1800061 (2018).
23. V. Bharadwaj, O. Jedrkiewicz, J. P. Hadden, B. Sotillo, M. R. Vázquez, P. Dentella, T. T. Fernandez, A. Chiappini, A. N. Giakoumaki, T. L. Phu, M. Bollani, M. Ferrari, R. Ramponi, P. E. Barclay, and S. M. Eaton, "Femtosecond laser written photonic and microfluidic circuits in diamond," J. Phys. Photonics **1**(2), 022001 (2019).
24. S. Lagomarsino, S. Sciortino, B. Obreshkov, T. Apostolova, C. Corsi, M. Bellini, E. Berdermann, and C. J. Schmid, "Photoionization of monocrystalline CVD diamond irradiated with ultrashort intense laser pulse," Phys. Rev. B **93**(8), 085128 (2016).
25. T. V. Kononenko, M. Meier, M. S. Komlenok, S. M. Pimenov, V. Romano, V. P. Pashinin, and V. I. Konov, "Microstructuring of diamond bulk by IR femtosecond laser pulses," Appl. Phys. A **90**(4), 645–651 (2008).
26. S. Kroesen, W. Horn, J. Imbrock, and C. Denz, "Electro–optical tunable waveguide embedded multiscan Bragg gratings in lithium niobate by direct femtosecond laser writing," Opt. Express **22**(19), 23339–23348 (2014).
27. F. Chen and J. R. V. de Aldana, "Optical waveguides in crystalline dielectric materials produced by femtosecond-laser micromachining," Laser Photonics Rev. **8**(2), 251–275 (2014).
28. A. Couairon and A. Mysyrowicz, "Femtosecond filamentation in transparent media," Phys. Rep. **441**(2-4), 47–189 (2007).
29. Y. C. Chen, P. S. Salter, S. Knauer, L. Weng, A. C. Frangeskou, C. J. Stephen, S. N. Ishmael, P. R. Dolan, S. Johnson, B. L. Green, G. W. Morley, M. E. Newton, J. G. Rarity, M. J. Booth, and J. M. Smith, "Laser writing of coherent colour centres in diamond," Nat. Photonics **11**(2), 77–80 (2017).
30. J. P. Hadden, V. Bharadwaj, B. Sotillo, S. Rampini, R. Osellame, J. D. Witmer, H. Jayakumar, T. T. Fernandez, A. Chiappini, C. Armellini, M. Ferrari, R. Ramponi, P. E. Barclay, and S. M. Eaton, "Integrated waveguides and deterministically positioned nitrogen vacancy centers in diamond created by femtosecond laser writing," Opt. Lett. **43**(15), 3586–3589 (2018).